Glasnik hemičara i tehnologa Bosne i Hercegovine

Bulletin of the Chemists and Technologists of Bosnia and Herzegovina

2026

66

23-30

Print ISSN: 0367-4444
Online ISSN: 2232-7266

Original Scientific Article
DOI: 10.35666/2232-7266.2026.66.03
UDK: 544.272:004

Monte Carlo Simulation of a Seeded Growth Model on a Triangular Lattice: Impact of Surface Impurities on the Final Morphology

Dujak, D. [a,*], Karač, A.[b]

[a] *Faculty of Electrical Engineering, University of Sarajevo, Zmaja od Bosne bb., Kampus Univerziteta, 71 000 Sarajevo, Bosnia and Herzegovina*
[b] *Polytechnic Faculty, University of Zenica, Fakultetska 1, 72 000 Zenica, Bosnia and Herzegovina*

Article info
Received: 09/12/2025
Accepted: 05/03/2026

Keywords:
Jamming
Seeded growth
Impurities
Triangular lattice
RSA

***Corresponding author:**
Dijana Dujak
E-mail: ddujak@etf.unsa.ba
Phone: +-387 33 250 770

Abstract: This study investigates the influence of surface contamination on the final morphology generated by a seed-mediated growth model on a two-dimensional triangular lattice. Using Monte Carlo simulations, we examine the interplay between growth rules (specifically rigid k-mer extension and flexible self-avoiding random walk (SARW) chains) and the geometric properties of pre-adsorbed impurities. Contrary to the initial hypothesis of a geometric matching between the growing species and the surface impurities, our results show that the final morphology in the jamming state is remarkably insensitive to the local symmetry or compactness of the impurities. For rigid k-mers, growth arrest is primarily driven by the impurity number density, which overrides any potential advantages of linear alignment with specific defect shapes. For SARW chains, the available void space and its topological connectivity limit the length, overshadowing the advantages of impurity compactness. Our findings reveal structural robustness in surface growth processes, where intrinsic growth rules dictate length scales, but the overall impurity coverage governs the overall feature distribution. This suggests that morphological outcomes are predictable based on total contamination levels, offering a simplified framework for controlling the growth of nanostructures in realistic, inhomogeneous environments.

INTRODUCTION

Understanding particle adhesion and growth on surfaces is fundamental to processes such as heterogeneous catalysis and electrodeposition, where the final morphology dictates the efficiency and connectivity of the system (Adamczyk, 2006). In these systems, deposition often occurs irreversibly on the experimental time scale, making the Random Sequential Adsorption (RSA) model a robust framework for describing the resulting configurations (Privman, 2000; Cadilhe, 2007). RSA is a process in which objects are deposited randomly and sequentially on a substrate (Talbot, 2000). In its simplest form, the RSA model does not allow for overlapping of objects. Once deposited, the objects remain permanently fixed and affect the geometry of all subsequent depositions. During RSA, the number of deposited objects increases over time. The fraction of the substrate area covered by adsorbed objects, called the coverage fraction $\theta(t)$, describes the kinetic properties of the deposition process. The process stops when there is not enough space for another object. This state is called the jamming state, in which the coverage fraction reaches its jamming limit θ_J. It represents the final configuration of the surface covered by adsorbed objects (Perino, 2017; Ramirez-Pastor, 2019).

In the last twenty years, a variety of nanoscale building blocks of controlled size, shape, and structure have been synthesized for use in fields such as chemical engineering, medicine, and electronics. Seed growth has been shown to be effective for the production of diverse metal nanostructures suitable as substrates for further material deposition (Gole, 2004; Habas, 2007; Lohse, 2013; Xia, 2017). The model proposed in (Dujak, 2022) simulates granular growth on a triangular lattice, allowing different forms of growth without restrictions. It considers the simultaneous development of multiple finite clusters, with the initial seed concentration serving as an adjustable parameter (Roy, 2017). The jamming limit θ_J is reached

when none of the growing objects can propagate further in any required direction on the lattice.

While early models assumed spatially homogeneous substrates (Evans, 1993), real chemical surfaces are inherently inhomogeneous due to the presence of adsorbed pollutants, vacancy defects, or intentional dopants (Adamczyk, 2005; Weroński, 2005). For example, the synthesis of 2D nanomaterials and graphene nanoribbons on Au (111) or Ni (111) is strongly influenced by surface defects. Prominent examples include the growth of nitrogen (Usachov et al., 2011) and boron (Gebhardt et al., 2013) doped graphene on Ni (111), where foreign atoms on the triangular lattice change the electronic properties and network connectivity. Furthermore, the specific configuration of adsorbate, such as gold clusters, can tune the doping characteristics of the material (Wu et al., 2012). These systems demonstrate how surface inhomogeneities, whether point-like or extended, govern the morphological characteristics of the deposited phase (Vasudevan, 2019). In modelling such processes, heterogeneity is introduced by initially occupying lattice sites with objects representing localized chemical defects (Centres, 2015).

In this paper, we investigate the final surface morphology and covering structures generated by a particle-seeded growth model on a two-dimensional triangular lattice initially occupied by impurities. Instead of treating impurities as point-like obstacles, we examine how their shape (defined by internal symmetry and compactness**)** affects the final morphology in the jamming state. Our study is designed to test a central hypothesis about the morphological properties of the final lattice covering in the jamming state, with a particular focus on geometric matching and compactness. For rigid, needle-like growth (k-mers), we hypothesize that the final length distribution will be sensitive to the impurity shape; specifically, that linear impurities will align more favourably with the k-mer growth rules, leaving open pathways that allow for longer objects compared to angular or bent impurities. For flexible growth, we expect that more compact impurities with higher symmetry will lead to more interconnected coverings and longer chains by concentrating the excluded volume, thus preserving wider continuous corridors on the lattice. By analysing the resulting object length distributions, we aim to determine whether the local geometry of the surface contamination is a key design parameter. This investigation is motivated by previous findings (Dujak, 2024) that showed that, although the percolation threshold is sensitive to the shape of the impurity, the overall jamming limit remains largely invariant. Here, we aim to determine whether this invariance extends to the local morphological level or whether the intrinsic growth rules of the species play a more dominant role in shaping the final morphology**.**

EXPERIMENTAL

Definition of the model and the simulation method

The substrate for seed growth is a two-dimensional triangular lattice of size $L = 3200$. To minimize edge effects and simulate an infinite surface, periodic boundary conditions are applied to the triangular lattice (i.e. sites on an open border are connected to corresponding sites on the opposite border). This approach is standard in surface science modelling because it ensures that each lattice site experiences a statistically equivalent environment, preventing artificial nucleation at the boundaries (Binder, 2010). Furthermore, the choice of lattice size $L = 3200$ was made to mitigate finite-size effects (Evans, 1984; Lebovka, 2011). In percolation and jamming studies, the size of the system can significantly affect the observed thresholds; however, for the densities and object lengths considered here ($l = 2$), $L = 3200$ is large enough to ensure that morphological statistics (such as length distributions and jamming limits) are representative of the thermodynamic limit and are not biased by the size of the system.

The lattice was initially and randomly populated with impurities using RSA. They are created by self-avoiding random walks of length $l = k - 1$, where k represents the number of the occupied lattice sites. Three shapes of such impurities are possible, as shown in Table 1. The impurity concentrations ρ_{imp} were kept below the percolation threshold of the triangular lattice sites (given in Table 1) to ensure that the substrate remained a connected medium, allowing unhindered growth paths before the jamming state. Later, point seeds were randomly distributed on the lattice at a given concentration ρ. To ensure the physical validity of the results, the initial seed concentrations were also intentionally kept below the percolation threshold of the sites for point objects on the triangular lattice ($p_c = 0.5$). This constraint ensures that any connectivity or percolation observed in the jamming state is a direct consequence of the growth process and its interaction with the impurities, and not a by-product of the initial distribution. Seed and impurity concentrations are calculated as the fraction of lattice sites occupied by seeds/impurities.

Table I: Formation of impurities of the length $l = 2$ with corresponding order of the symmetry axis of the shape *n*, jamming coverages θ_J and percolation thresholds θ_p. The numbers in parentheses are the numerical values of the standard uncertainty of θ_J referred to the last digits of the quoted value.

Impuritiy shapes	*n*	θ_J	θ_p
(B)	2	0.836 211(4)	0.4611(9)
(C) 	1	0.834 440(4)	0.4585(11)
(D) 	3	0.796 940(5)	0.5214(9)
(B) + (C)	/	0.8525(7)	0.4587(12)
(B) + (D)	/	0.8588(6)	0.4926(12)
(C) + (D)	/	0.8625(7)	0.4910(12)

Seed growth on a lattice is modelled using self-avoiding walks, following two distinct growth rules: (i) unidirectional growth, which results in rigid, needle-like structures (k-mers), and (ii) isotropic growth, where flexible chains (SARW) are formed. During object growth, objects come into contact when there is one lattice site between them, and merged into a single cluster. If two

clusters come into contact, they merge into a single cluster. The jamming coverage θ_J is reached when growing objects can no longer grow on the lattice.

The simulation proceeds until a jamming state is reached. Physically, this corresponds to the surface saturation limit where the available free volume is fragmented into domains smaller than the minimum size of the growing species. This state provides a well-defined point for morphological analysis, representing the final stage of kinetic growth before any potential (and often much slower) thermal reorganization takes place.

Simulation method

The lattice is initially randomly occupied by impurities B, C or D or by their mixtures B+C, B+D and C+D at a given concentration ρ_{imp}, and then by point seeds randomly distributed at a given concentration ρ. Then, the deposition is turned off, and the process of random growing begins. In each Monte Carlo step, the lattice site occupied by the seed is randomly selected. After that, an unoccupied adjacent site is randomly selected according to the prescribed growth rules for the seed. In the case of needle-like growth, the selected k-mer extends in the direction of the first step in the formation of the growing object. If the corresponding adjacent site is occupied by an impurity or a previously grown object, the attempted k-mer growth is not possible and the object remains unchanged. In the case of flexible chains, the selected chain is randomly extended to one of the nearest empty neighbour sites. If all the nearest neighbour sites are occupied, the selected chain is not changed. During the process, the lattice coverage increases up to the jamming limit.

Chemical relevance and model limitations

The Monte Carlo model presented provides a theoretical framework for understanding how surface contamination affects the final lattice morphology. Although defined on a discrete triangular lattice, the model rules and parameters are specifically chosen to reflect the physical and chemical constraints of real-world surface processes.

The choice of a triangular lattice is physically justified by the (111) facet of face-centered cubic (fcc) metals (e.g., Au, Pt, Ag), which serve as the most common substrates for on-surface synthesis (Brune, 1998; Poirier, 1997; Kawasaki, 2006). In this context, the growing species serve as analogs for different classes of organic molecules. For example, rigid k-mers can represent conjugated rod-like molecules (Kondrat, 2001; Kondrat, 2002; Adamczyk, 2008), while SARW chains can model flexible polymers (oligomers) or long-chain alkanes with conformational degrees of freedom (Cornete, 2003; Pawłowska, 2012). Furthermore, the impurities of length l=2 represent the minimal extended defects, such as pre-adsorbed diatomic molecules or vacancy clusters, which introduce localized steric hindrance beyond simple point-like poisoning (Weroński, 2005).

The assumption of irreversible growth without surface diffusion is a well-established theoretical framework in the study of non-equilibrium deposition. As discussed by Privman (2000), the irreversible RSA model without detachment or diffusion leads to a fully jammed state where the coverage is limited by the exclusion of particles from gaps smaller than their size. Our model follows this established methodology to isolate the influence of geometric constraints and surface impurities on the final morphology.

The central assumption of our study is the dominance of excluded volume effects. In many chemical synthesis processes, especially under high surface coverage, steric constraints impose fundamental limits on growth and dictate the final morphology. This behavior is well-documented in self-assembled monolayers and colloidal nanocrystal assembly, where short-range steric repulsion, rather than long-range electrostatic forces, governs particle organization and packing boundaries (Boles, 2016).

Recent theoretical models of the seed-mediated growth, such as mean-field analytical studies of nanodiamond film formation as a function of seed density and initial seed size, confirm that the spatial distribution and hard-core interactions of the seeds are the primary drivers of the transition to continuous coverage (Tomellini, 2023). By focusing on these hard-core interactions, our model captures the essential physics of crowding observed in dense deposition regimes. This justifies the use of a simplified lattice model where steric repulsion and spatial accessibility are the primary controlling mechanisms for nanostructural engineering.

RESULTS AND DISCUSSION

The final morphology was tested in the jamming state for various seed concentrations $(0.1 \leq \rho \leq 0.49)$ on a triangular lattice of size $L = 3200$, and for different impurity concentrations $(0.1 \leq \rho_{imp} \leq 0.48)$ in the case of individual impurities. For impurity mixtures, the ranges were $(0.1 \leq \rho \leq 0.48)$ and $(0.1 \leq \rho_{imp} \leq 0.35)$. The data were averaged over 500 independent runs. To investigate the morphology, we consider the number of objects $N = N(l)$, $l \geq 0$, normalized by the initial number of seeds N_0 for k-mers and SARW, and analysed for different values of ρ and ρ_{imp}.

The dependence of the ratio N/N_0 on the k-mer length for the system in the jamming state is shown in Fig. 1 and Fig. 2 for various values of the seed density ρ and all three types of impurities given in Table 1. The results for a low value of ρ_{imp} are presented in Fig. 1 while Fig. 2 shows the results for high impurity concentrations. A comparative analysis of these figures reveals a striking similarity in the morphological evolution of the growing objects, regardless of the specific internal symmetry or compactness of the impurities. It is important to note that for a fixed impurity density, the total number of impurities remains constant in all studied cases; consequently, the number density of the impurities, is identical. Our results show that at low concentrations, the final morphology is primarily determined by this number density and the resulting total excluded volume. The specific internal symmetry of the impurities (whether linear or angular) represents a second-order effect that does not significantly change the statistical distribution of the grown k-mers.

In all cases, as the seed density increases, we observe a sharp transition where the peak of the distribution shifts towards $l = 1$ (monomers). At $\rho = 0.45$, approximately

60% of the seeds do not pass a single growth step. This growth inhibition is a manifestation of the crowding effect, driven by competition for excluded volume; at high seed densities, the available lattice space is partitioned into domains smaller than the required propagation length, leading to premature jamming. There is a distinct overlap point at $l = 2$. For lengths $l > 2$, the probability of reaching longer lengths drops significantly faster for higher seed densities.

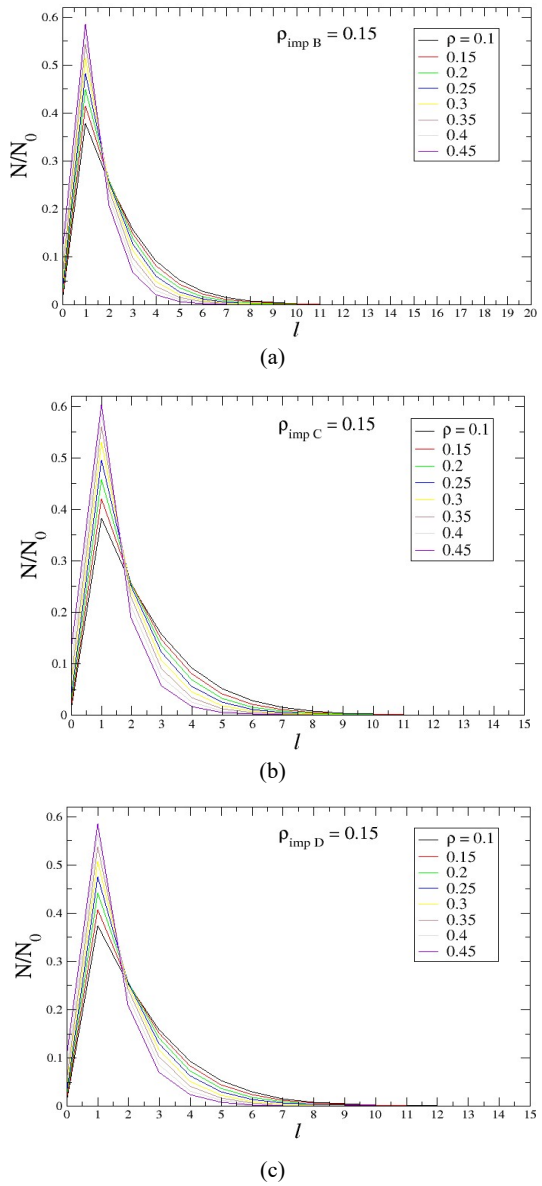

Fig 1: The dependence of the normalized number of growing k-mers on their length in the jamming state for low impurity concentration. The specific types of impurities (B, C, D), their concentrations (ρ_{imp}), and the initial seed concentrations (ρ) are indicated in the legend.

Under the conditions of extreme surface contamination, the growth process is severely hindered, as evidenced by the almost complete suppression of k-mer extension above $l = 2$. A critical observation is the collapse of the length distribution towards $l = 1$. For high seed densities ($\rho > 0.35$), the fraction of non-growing seeds exceeds 60%, representing a state of premature jamming. In this regime, the surface is so heavily fragmented by pre-adsorbed impurities that the connectivity of the triangular lattice is effectively destroyed. The fact that the distributions for shapes B, C, and D remain indistinguishable even at such high densities suggests that vacancy percolation is the fundamental phenomenon governing the morphology, rather than a specific interaction between the growth species and the impurity geometry.

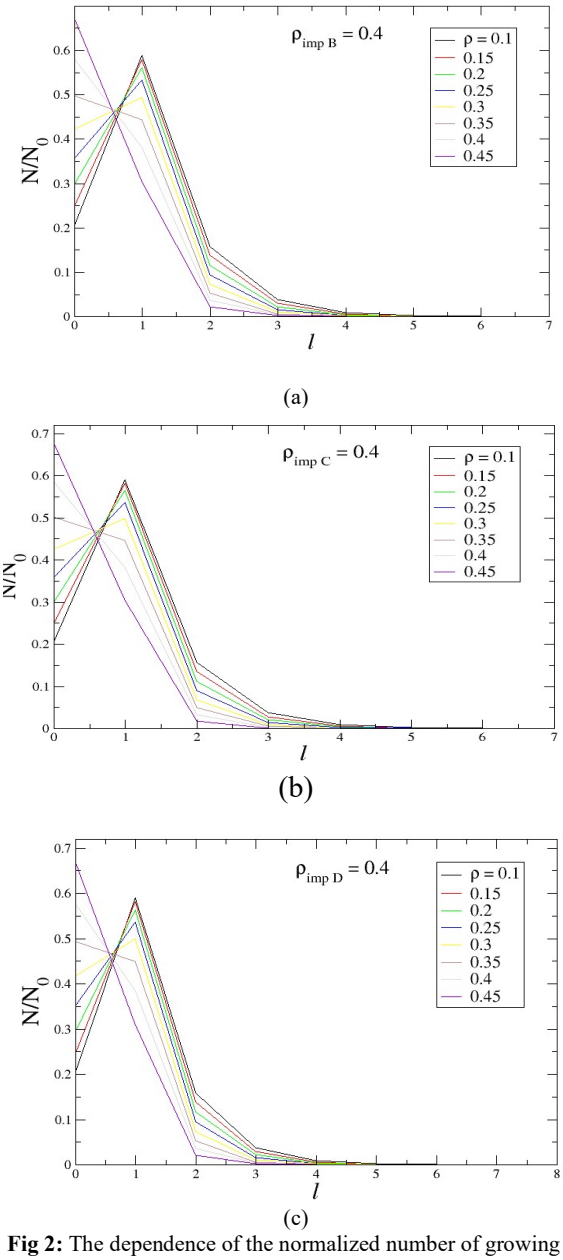

Fig 2: The dependence of the normalized number of growing k-mers on their length in the jamming state for high impurity concentration. The specific types of impurities (B, C, D), their concentrations (ρ_{imp}), and the initial seed concentrations (ρ) are indicated in the legend.

The corresponding results for random walk chains (SARW) are shown in Fig. 3 for low impurity concentrations and in Fig. 4 for high impurity concentrations. Unlike rigid k-mers, SARW chains

achieve significantly larger maximum lengths, often exceeding $l > 20$ at low ρ and ρ_{imp}. This advantage of SARW chains over k-mers highlights the role of conformational freedom in overcoming steric hindrance; while rigid k-mers are easily blocked by a single pinning site, the flexible nature of SARW allows for the exploration of a larger fraction of the available free volume.

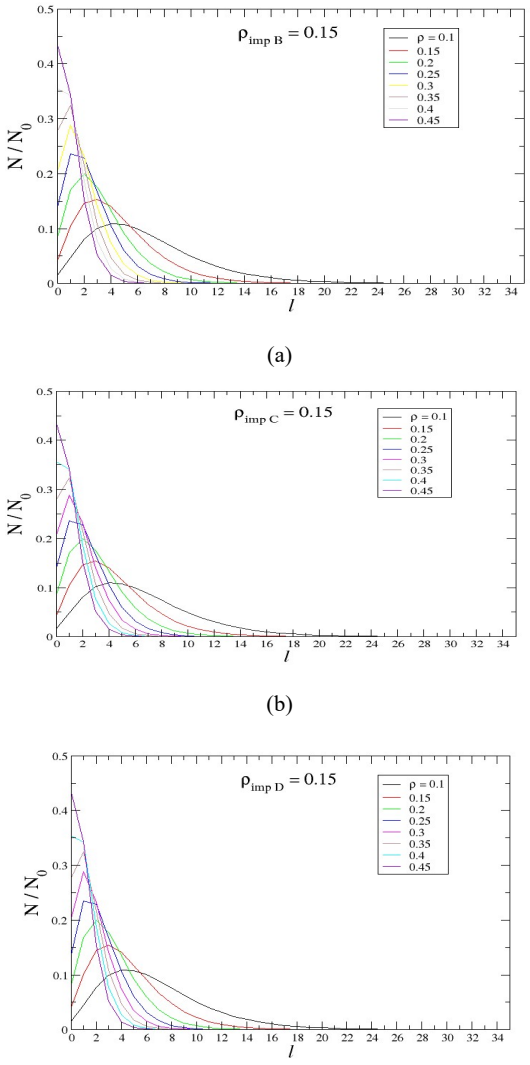

Fig 3: The dependence of the normalized number of growing SARW chains on the walk length in the jamming state for low impurity concentration. The specific types of impurities (B, C, D), their concentrations (ρ_{imp}), and the initial seed concentrations (ρ) are indicated in the legend.

At low impurity concentrations, the distribution peak shifts towards higher l values compared to k-mers, indicating that flexible growth is less sensitive to low-level surface contamination. However, as ρ and ρ_{imp} increase, this advantage decreases. The suppression of vacancy percolation at high impurity densities effectively limits the available free volume, leading to the observed growth suppression even for flexible SARW chains. At high impurity and seed densities, the system eventually converges to the behaviour observed for k-mers. This convergence occurs because the lattice fragments into geometric domains smaller than the typical persistence length of even a flexible chain, making the configurational flexibility of SARW ineffective against such severe spatial constraints.

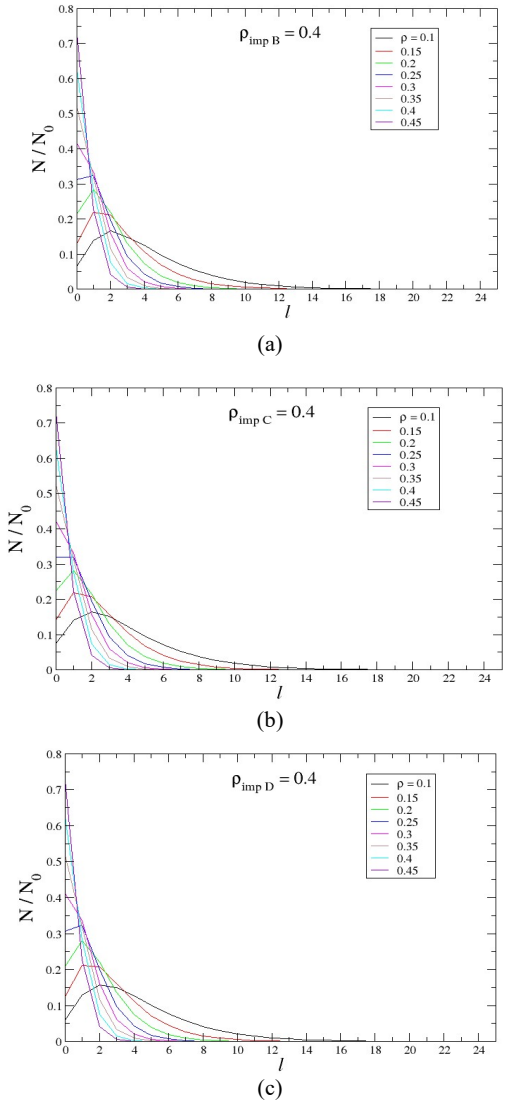

Fig 4: The dependence of the normalized number of growing SARW chains on the walk length in the jamming state for high impurity concentration. The specific types of impurities (B, C, D), their concentrations (ρ_{imp}), and the initial seed concentrations (ρ) are indicated in the legend.

Figures 5 and 6 show the normalized object length distribution for all types of impurities listed in Table 1 and their mixtures. For comparison, results for point-like impurities (k-mers with $l = 0$) and for growth without impurities are also included. Specifically, Fig. 5a presents the results for low densities of both impurities and seeds, while Fig. 5b corresponds to low impurity density and high seed density. Conversely, Figs. 6a and 6b illustrate the opposite cases. The corresponding results for SARW chains are given in Figs. 7 and 8.

The results in Figs. 5a and 5b show that, for low values of impurity and seed densities, the length distributions of the growing objects are almost identical for all impurity shapes and their mixtures.

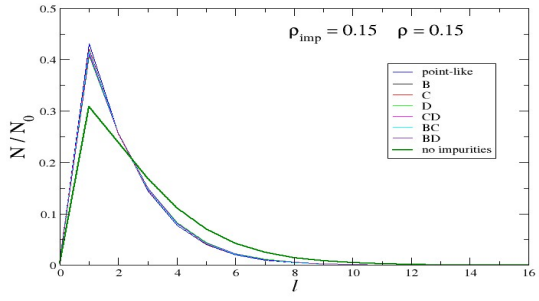

(a)

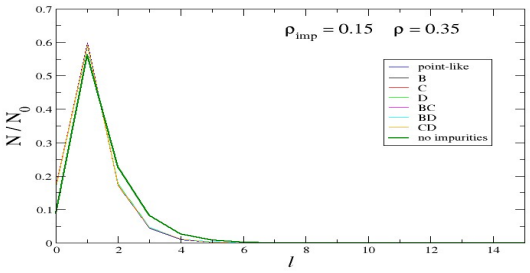

(b)

Figure 5: Comparison of object length distributions in the jamming state during k-mer growth at low impurity densities ($\rho_{imp} = 0.15$) and (a) low seed densities ($\rho = 0.15$), (b) high seed densities ($\rho = 0.35$). The type of impurities is indicated in the legend. For comparison, results for k-mer growth without impurities are also shown.

The objects attain slightly shorter lengths compared to the case without impurities, indicating a minimal but measurable steric disruption. Notably, at high seed densities and low impurity concentrations, the distributions match those observed for growing on a pure lattice. This suggests that in the high-seed regime, the inter-seed competition (the crowding effect) becomes the primary limiting factor for growth. In this scenario, the high frequency of collisions between adjacent growth fronts effectively masks the presence of rare impurities**,** as growing objects exhaust the available lattice space before they can significantly interact with the pre-adsorbed obstacles.

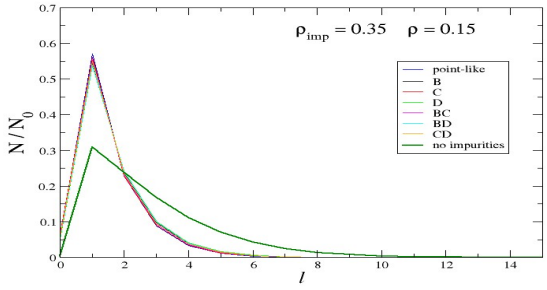

(a)

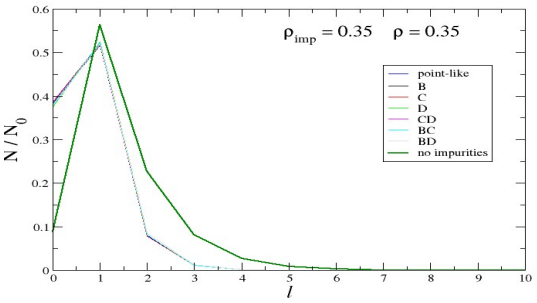

(b)

Figure 6: Comparison of object length distributions in the jamming state during k-mer growth at high impurity densities ($\rho_{imp} = 0.35$) and (a) low seed densities ($\rho = 0.15$), (b) high seed densities ($\rho = 0.35$). The type of impurities is indicated in the legend. For comparison, results for k-mer growth without impurities are also shown.

In contrast, Figs. 6a and 6b show that, at high impurity concentrations, the objects in the jamming state reach significantly shorter lengths than in the case of no-impurities. In this regime, the growth suppression is primarily caused by strong lattice fragmentation; the high density of impurities acts as a decisive barrier to chain elongation, regardless of their specific geometry.

From the growth of SARW chains shown in Figs. 7 and 8, it can be concluded that, in general, longer objects are formed compared to the growth of *k*-mers under the same conditions.

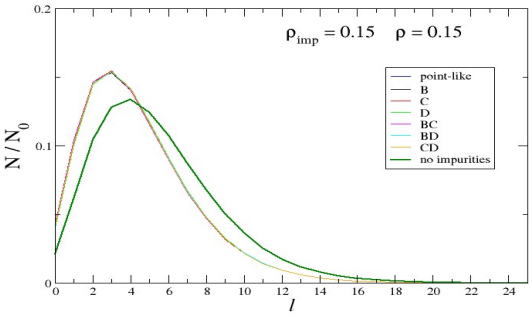

(a)

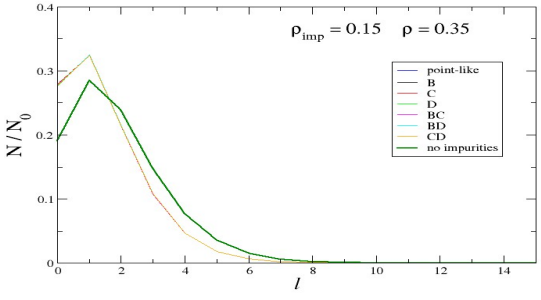

(b)

Figure 7: Comparison of object length distributions in the jamming state during SARW chains growth at low impurity densities ($\rho_{imp} = 0.15$) and (a) low seed densities ($\rho = 0.15$), (b) high seed densities ($\rho = 0.35$). The type of impurities is indicated in the legend. For comparison, results for SARW chains growth without impurities are also shown.

At low impurity densities, the length distributions remain remarkably consistent across all impurity shapes, deviating only slightly from the impurity-free case.

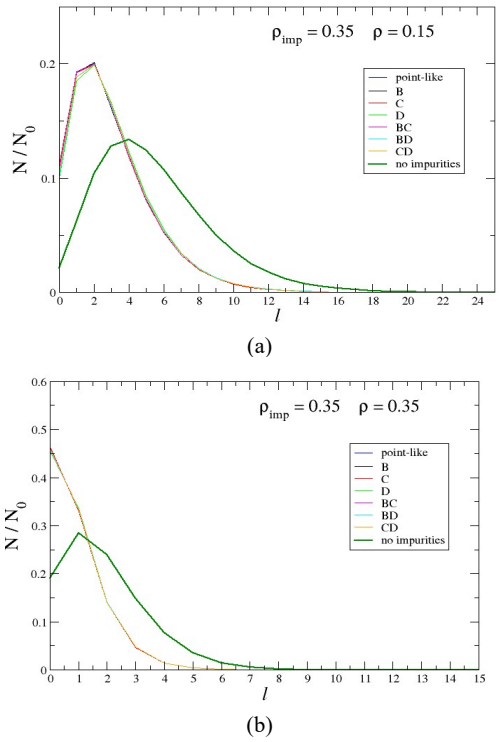

Fig 8: Comparison of object length distributions in the jamming state during SARW chains growth at high impurity densities ($\rho_{imp} = 0.35$) and (a) low seed densities ($\rho = 0.15$), (b) high seed densities ($\rho = 0.35$). The type of impurities is indicated in the legend. For comparison, results for SARW chains growth without impurities are also shown.

However, this difference becomes more pronounced at higher impurity and seed densities. In these crowded environments, growth on a clean lattice yields significantly longer chains and a lower fraction of non-growing seeds. This behaviour highlights a critical transition: while the conformational freedom of SARW chains allows them to bypass isolated obstacles, the cumulative effect of high impurity concentrations eventually leads to extreme spatial confinement. In such regimes, the impurities act as pinning sites that fragment the available growth paths into finite, isolated domains. This limits the achievable length of the flexible chains, as the probability of a random walk becoming trapped within a small empty pocket increases, ultimately reducing the morphological advantage of flexible species over rigid k-mers.

CONCLUSIONS

This study systematically assessed the influence of impurity geometry on the seeded growth of rigid k-mers and flexible SARW chains. Our findings provide a clear solution to the central hypothesis proposed in the introduction: contrary to our initial assumption, the final morphology in the jamming state is remarkably insensitive to the local geometric matching between the impurities and the growing species.

For rigid k-mers, we assumed that linear impurities would align with growth paths to allow for longer objects; however, our results reveal that the number density of impurities is the primary driver of growth arrest. The expected advantage of linear alignment is effectively negated by the stochastic nature of seed placement, which fragments the lattice regardless of the specific impurity symmetry. Similarly, for flexible SARW chains, the expected benefit of compact impurities with higher symmetry order preserving wider corridors was not observed. Instead, we found that at the concentrations studied, the percolation of void space (the global connectivity of empty sites) acts as the fundamental limiting factor, overshadowing any local advantages provided by impurity compactness. This work has demonstrated a geometric universality in surface growth, where the intrinsic growth rules (rigidity vs. flexibility) dictate the absolute length scales, but the total impurity coverage – rather than their specific shape – governs the statistical distribution of the grown objects.

These insights are particularly relevant for experimental nano-deposition on substrates like Au (111). They suggest that the morphological outcome of surface coatings is a robust property that can be predicted based on the overall level of contamination, without the need for detailed characterization of defect symmetries. This robustness simplifies the design parameters for controlling surface growth in non-ideal, realistic environments.

REFERENCES

Adamczyk Z., Jaszczt K., Michna A., Siwek B., Szyk-Warszyska L., Zembala M. (2005). Irreversible adsorption of particles on heterogeneous surfaces, *Adv. Colloid Interface Sci. 118*, 25–42.

Adamczyk Z. (2006). Particles at Interfaces: Interactions, Deposition, Structure, Interface Science and *Technology 9*, 1-743.

Adamczyk P., Romiszowski P. Sikorski A. (2008). A simple model of stiff and flexible polymer chain adsorption: The influence of the internal chain architecture, *J. Chem. Phys. 128*, 154911.

Binder K., Heermann D.W. (2010). Monte Carlo simulations in Statistical physics, 5th edition, Springer.

Boles M. A., Engel M., Talapin D. V. (2016). Self-Assembly of Colloidal Nanocrystals: From Intricate Structures to Functional Materials, *Chemical Reviews 116*, 11220–11289.

Brune H. (1998). Microscopic view of epitaxial metal growth: nucleation and aggregation, *Surface Sci. Rep. 31*, 125-229.

Cadilhe A., Araujo N. A., Privman V. (2007). Random sequential adsorption: from continuum to lattice and pre-patterned substrates, *J Phys.: Condens. Matter 19,* 065124.

Centres P. M., Ramirez-Pastor A. J. (2015). Percolation and jamming in random sequential adsorption of linear k-mers on square lattices with the presence of impurities, *J. Stat. Mech. 2015*, 10011.

Cornette V., Ramirez-Pastor A. J., Nieto F. (2003). Dependence of the percolation threshold on the size of the percolating species, *Physica A 327*, 71.

Dujak D. et al. (2022). Percolation and jamming properties in particle shape-controlled seeded growth model, *Eur. Phys. J. B 95*, 143.

Dujak D. et al. (2024). Percolation and jamming properties in an object growth model on a triangular lattice with finite-size impurities, *J. Stat. Mech. 2024,* 1742–5468.
Evans J. W., Burgess D. R., Hoffman D. K. (1984). Irreversible random and cooperative processes on lattices: spatial correlations, *J. Math. Phys. 25*, 3051–63.
Evans J. W. (1993). Random and cooperative sequential adsorption, *Rev. Mod. Phys. 65*, 1281.
Gebhardt J. et al. (2013). Growth and electronic structure of boron-doped graphene*, Phys. Rev. B* 87, pp. 155437.
Gole A., Murphy C. J. (2004). Seed-Mediated Synthesis of Gold Nanorods: Role of the Size and Nature of the Seed, *Chem. Mater. 16*, 3633–3640.
Habas S. E. et al. (2007). Shaping binary metal nanocrystals through epitaxial seeded growth, *Nature Materials 6,* 692–697.
Kawasaki M., Masaki I. (2006). Self-Assembly of Alkanethiol Monolayers on Ag−Au (111) Alloy Surfaces, *The Journal of Physical Chemistry B 110*, 21124–21130.
Kondrat G., Pekalski A. (2001). Percolation and jamming in random bond deposition, *Phys. Rev. E 64*, 056118.
Kondrat C. (2002). Influence of temperature on percolation in a simple model of flexible chains adsorption, *J. Chem. Phys.* 117, pp. 6662–6666.
Lebovka N. I., Karmazina N. N., Tarasevic Y. Y., Laptev V. V. (2011). Random sequential adsorption of partially oriented linear k-mers on a square lattice, *Phys. Rev. E 84*, 061603.
Lohse S.E., Murphy C. J. (2013). The quest for shape control: a history of gold nanorod synthesis, *Chem. Mater. 25*, 1250−61.
Pawłowska M., Żerko S., Sikorski, A. (2012). Percolation in two-dimensional flexible chains systems, *The Journal of Chemical Physics 136*, 046101.
Perino E. J., Matoz-Fernandez D. A., Pasinetti P. M., Ramirez-Pastor A. J. (2017). Jamming and percolation in random sequential adsorption of straight rigid rods on a two-dimensional triangular lattice. *J. Stat. Mech. 2017,* 073206.
Poirier G. E. (1997). Characterisation of Organosulfur Molecular Monolayers on Au (111) using Scanning Tunnelling Microscopy. *Chem. Rev.* 97, 1117-1128.
Privman V. (2000). Dynamics of Nonequilibrium Deposition, *Colloids Surf. A 165,* 231.
Ramirez-Pastor A. J., Centres P. M., Vogel E. E., Valdés J. F. (2019). Jamming and percolation for deposition of k^2-mers on square lattices: A Monte Carlo simulation study, *Phys. Rev. E 99*, 042131.
Roy B., Santra S. B. (2017). First-order transition in a percolation model with nucleation and preferential growth, *Phys. Rev. E 95*, 010101.
Talbot J., Tarjus G., Van Tassel P. R., Viot P. (2000). From car parking to protein adsorption: an overview of sequential adsorption processes, *Colloids Surf. A 165*, 287–324.
Tomellini M., Polini R. (2023). Impact of seed density on continuous ultrathin nanodiamond film formation, *Diamond and Related Materials 133*, 109700.
Usachov D. et al. (2011). Nitrogen-Doped Graphene: Efficient Growth, Structure, and Electronic Properties, *Nano Letters 11*, 5401–5407.
Vasudevan A., Shvalya V., Zidanšek A., Cvelbar U. (2019). Tailoring electrical conductivity of two-dimensional nanomaterials using plasma for edge electronics: A mini review, *Front. Chem. Sci. Eng. 13*, 427–443.
Weroński P. (2005). Application of the extended RSA models in studies of particle deposition at partially covered surfaces, *Adv. Colloid Interface Sci. 118*, 1–24.
Wu Y. et al. (2012). Tuning the Doping Type and Level of Graphene with Different Gold Configurations*, Small 8,* 3129–3132.
Xia Y., Gilroy K. D., Peng H. C., Xia X. (2017). Seed-Mediated Growth of Colloidal Metal Nanocrystals, *Angewandte Chemie Int. Ed*. 56, 60–95.

AKNOWNLEDGEMENT

This paper emerged from the project number PtF_EM_IR_04/2024.

Summary/Sažetak

U ovom radu se istražuje uticaj površinske kontaminacije dvodimenzionalne triangularne rešetke na konačnu morfologiju površine rešetke formirane modelom rasta (seed-mediated growth). Koristeći Monte Carlo simulacije, ispitivan je uticaj pravila rasta (kruti k-meri i fleksibilni SARW lanci) i geometrijskih svojstava prethodno adsorbovanih nečistoća. Suprotno početnoj hipotezi o geometrijskom podudaranju nečistoća i objekata formiranih narastanjem, rezultati pokazuju da je konačna morfologija u stanju zagušenja (*jamming state*) izuzetno neosjetljiva na lokalnu simetriju ili kompaktnost nečistoća. Kod krutih k-mera, zaustavljanje rasta prvenstveno je uzrokovano brojčanom gustinom nečistoća, što nadjačava bilo kakve potencijalne prednosti linearnog poravnanja sa specifičnim oblicima defekata. Kod SARW lanaca, raspoloživi prazan prostor i njegova topološka povezanost ograničavaju dostižnu dužinu, zasjenjujući prednosti kompaktnosti nečistoća. Uočena je strukturna robusnost u procesima površinskog rasta, gdje unutrašnja pravila rasta diktiraju skale dužine, dok ukupna prekrivenost nečistoćama upravlja cjelokupnom distribucijom objekata. Ovo sugeriše da su morfološki ishodi predvidljivi na osnovu ukupnog nivoa kontaminacije, što nudi pojednostavljen okvir za kontrolu nanostrukturnog rasta u realnim, nehomogenim okruženjima.